Design and verification of a robust controller for the twin rotor MIMO system

Petr Chalupa, Jakub Novák, Jan Přikryl

***Abstract*—**The paper deals with control design and verification of a robust controller of the Twin Rotor MIMO System – a real-time laboratory plant by Feedback Ltd. The plant physical appearance as well as its behavior resembles a helicopter. It consists of two propellers individually controlled by external controller. An initial nonlinear mathematical model is derived using first principles modeling and further used for simulation verification of the designed controllers. Besides, several linear black box models are identified by applying various input courses to the plant. Resulting set of models is used for robust control design. The designed robust controllers with promising behavior in simulations are verified by real-time control of the laboratory model.

***Keywords*—**First principle modelling, Real-time control, Robust control

I. Introduction

MOST of current control algorithms are based on a model of a controlled plant [1]. It is obvious that some information about controlled plant is required to allow for design of a controller with satisfactory performance. A plant model can be also used to investigate properties and behavior of the modeled plant without a risk of damage or violating technological constraints of the real plant. The re two basic approaches of obtaining plant model: the black box approach and the first principles modeling (mathematical-physical analysis of the plant).

The black box approach to the modeling [2], [3] is based on analysis of input and output signals of the plant. The main advantage of the black box approach consists in the possibility of usage the same identification algorithm for wide set of various controlled plants [4], [5]. Contrary, the first principle modeling provides general models valid for whole range of plant inputs and states. A model is created by analyzing the modeled plant and combining physical laws [6]. But, there are usually many unknown constants and relations when performing analysis of a plant. Therefore first principle models are suitable for simple controlled plants with small number of parameters. First principle modeling can be also used for obtaining basic information about controlled plant (rage of gain, rank of suitable sample time, etc.). Some simplifications must be used to obtain reasonable results in more complicated cases. These simplifications must relate with the purpose of the model. The first principle modeling is also referred to as white box modeling.

The paper combines both methods. Basic relations between plant inputs and outputs are derived using first principles. The obtained model is further improved on the basis of measurements. This approach is known as grey box modeling [7]. The goal of the work was to obtain a mathematical model of the Twin Rotor MIMO System [8], design the model in MATLAB-Simulink environment and use this model for design of adaptive controller. The Twin Rotor MIMO System was developed by Feedback Instruments Ltd. and serves as a real-time model of nonlinear multidimensional system. A model, which represents the plant well, can considerably reduce testing time of different control approaches. Then only promising control strategies are applied to the real plant and verified.

The paper is focused on robust control design [9]. Robust control approach allows obtaining a stabilizing controller not only for a nominal controlled system but also for a wider set of controlled systems. The set can be defined in various ways. This paper deals with parametric uncertainty, namely interval uncertainty [10].

The paper is organized as follows. Section 2 presents the modelled system – Twin Rotor MIMO System. A derivation of the nonlinear model and its implementation in the MATLAB / Simulink environment carried out in Section 3. Robust control design is presented in Section 4. As a part of robust design, linear models of the two single input single output decoupled subsystems are identified and presented also in Section 4. The verification of the designed robust controller using both nonlinear Simulink model and the real-time laboratory plant is described in Section 5.

II. Twin Rotor MIMO System

A photograph of the Twin Rotor MIMO System is presented in Fig. 1. The system is used to demonstrate the

This work was supported by the Ministry of Education, Youth and Sports of the Czech Republic within the National Sustainability Programme project No. LO1303 (MSMT-7778/2014).

This work was supported by the European Regional Development Fund under the project CEBIA-Tech No. CZ.1.05/2.1.00/03.0089. This support is greatly acknowledged.

Petr Chalupa is with the Tomas Bata University in Zlin, Faculty of Applied Informatics, Regional Research Centre CEBIA-Tech, nam. T. G. Masaryka 5555, 760 01 Zlin, Czech Republic (phone: +420 57603 5316, e-mail: chalupa@fai.utb.cz).

Jakub Novák is with the Tomas Bata University in Zlin, Faculty of Applied Informatics, Regional Research Centre CEBIA-Tech (email: jnovak@fai.utb.cz).

Jan Přikryl studied master degree at the Tomas Bata University in Zlin, Faculty of Applied Informatics.

principles of a non-linear MIMO system, with significant cross-coupling. Its behavior resembles a helicopter but contrary to most flying helicopters the angle of attack of the rotors is fixed and the aerodynamic forces are controlled by varying the speeds of the motors. Significant cross-coupling is observed between the actions of the rotors, with each rotor influencing both angle positions [11].

There are two propellers driven by DC-motors at both ends of a beam, which is pivoting on its base. The joint allows the beam to rotate in such a way that its ends move on spherical surfaces. There is a counter-weight fixed to the beam and it determines a stable equilibrium position. The controls of the system are the motors supply voltages. The measured signals are position of the beam in the space, i.e. two position angles [12].

Fig. 1. Twin Rotor MIMO System.

III. Model of the Twin Rotor MIMO System

A nonlinear model of the plant is derived in this section. The model is based on first principle modeling [12], [13], and [14]. More details concerning modeling of the Twin Rotor MIMO System can be found in [15].

There are two outputs of the plant: position angle in the vertical plane – elevation (i.e. angle with respect to horizontal axis) and position in the horizontal plane – azimuth (i.e. angle with respect to vertical axis). First vertical plane will be considered, and then the horizontal angle will be focused on. A schematic front view of the free beam and connected parts of the Twin Rotor MIMO System is depicted in Fig. 2. The gravitation forces taking effect are presented as well.

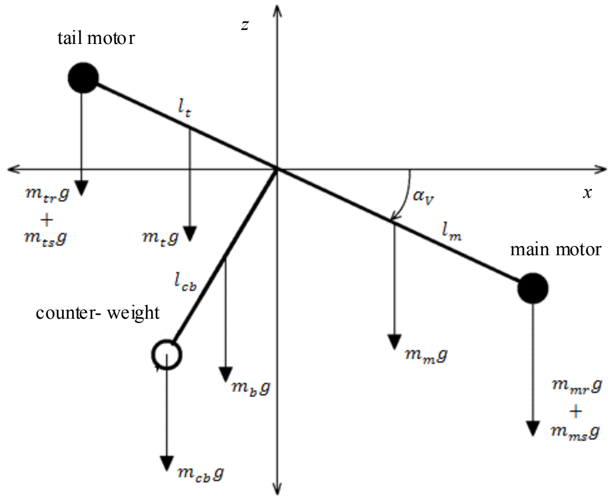

Fig. 2. Schematic front view of the Twin Rotor MIMO System with gravitation forces.

Constant g represents gravitational acceleration, parameters l_t, l_m and l_{cb} stand for the length of the tail part of the beam, the length of the main part of the beam and the length of the counter-weight beam respectively. The mass of the tail motor with tail rotor, the mass of the tail shield and the mass of the tail part of the beam are represented by m_{tr}, m_{ts}, and m_t respectively. Constants m_b and m_{cb} represent the mass of the counter-weight beam and the mass of the counter-weight respectively. The mass of the main motor with tail rotor, the mass of the main shield and the mass of the main part of the beam are represented by m_{mr}, m_{ms}, and m_m respectively. Finally α_v stands for the pitch angle of the beam – elevation

A. Initial model

The derivation of moments in the vertical plane is based on Newton's second law of motion:

$$M_v = J_v \frac{d^2\alpha_v}{dt} \tag{1}$$

where M_v is a sum of components of moment of forces and J_v is a sum of moments of inertia relative to horizontal axis of individual parts of the plant:

$$M_v = \sum M_{vi} \tag{2}$$

$$J_v = \sum J_{vi} \tag{3}$$

The moments present in the horizontal plane can be derived in the similar way as the moments in the horizontal plane.

It is possible to derive state equations of the whole system:

$$\frac{dS_v}{dt} = \frac{g\left[\left(A-B\right)\cos\alpha_v - C\sin\alpha_v\right] + l_m F_v\left(\omega_m\right)}{J_v} - \frac{\frac{1}{2}\Omega_h^2\left(A+B+C\right)\sin 2\alpha_v + \Omega_v k_v}{J_v} \tag{4}$$

$$\frac{dS_h}{dt} = \frac{l_t F_h(\omega_t)\cos\alpha_v - \Omega_h k_h}{J_h} \quad (5)$$

$$\Omega_v = S_v + \frac{J_{tr}\omega_t}{J_v}; \ \Omega_h = S_h + \frac{J_{mr}\omega_m \sin\alpha_v}{J_v} \quad (6)$$

where A, B, and C are constants derived from the physical parameters of the plant; S_v and S_h are the angular momentum in vertical plane for the beam and the angular momentum in horizontal plane for the beam respectively. The moment of inertia in DC-motor – tail propeller subsystem and the moment of inertia in DC-motor – main propeller subsystem are represented by J_{tr} and J_{mr} respectively.

These equations describe dependence of output angles (elevation α_v and azimuth α_h) on rotations of the main and the tail motors – ω_m and ω_t respectively. The motors are controlled by control voltage according to the following combinations of linear dynamics and static non-linearity:

$$\begin{aligned} \frac{du_{vv}}{dt} &= \frac{1}{T_{mr}}\left(-u_{vv} + u_v\right), \\ \omega_m &= P_v\left(u_{vv}\right) \end{aligned} \quad (7)$$

$$\begin{aligned} \frac{du_{hh}}{dt} &= \frac{1}{T_{tr}}\left(-u_{hh} + u_h\right), \\ \omega_t &= P_h\left(u_{hh}\right) \end{aligned} \quad (8)$$

where T_{mr} and T_{tr} are the time constant of the main motor – propeller system and the time constant of the tail motor – propeller system. Functions $P_v()$ and $P_h()$ describe the static nonlinearity of the main motor – propeller system and the static nonlinearity of the tail motor – propeller system. Inputs u_v and u_h represent the control voltage of the maim motor and the control voltage of the tail motor respectively.

B. Enhanced model

Documentation [12] provides parameters and relations of the Twin Rotor MIMO System which were presented in previous subsection. However real-time experiments showed that these parameters and equations should be refined or revised. This subsection is focused on modification of the initial model and parameters given in [12] in order to obtain better correspondence of the mathematical model and real time system.

1) Refinement of the dimensions

The dimensions of the modeled Twin Rotor MIMO System were measured to refine constants given in documentation [12]. Especially the length of the counter-weight beam is different from the value given in documentation.

2) Nonlinear static functions

The mode contains several nonlinear functions – e.g. equations (4), (5), (7) and (8). These functions have to be determined to design the final model. A phenomenological approach was used for their identification. A polynomial approximation was used without deep study of the physical fundamentals of the relation:

$$\begin{aligned} P_v\left(u_{vv}\right) &= 90.99u_{vv}^6 + 599.73u_{vv}^5 - 126.26u_{vv}^4 - \\ &\quad -1238.64u_{vv}^3 + 63.45u_{vv}^2 + 1283.41u_{vv} \end{aligned} \quad (9)$$

$$\begin{aligned} F_v\left(\omega_m\right) &= 3.187\cdot10^{-12}\omega_m^5 - 4.096\cdot10^{-9}\omega_m^4 + \\ &\quad +1.385\cdot10^{-6}\omega_m^3 + 1.234\cdot10^{-2}\omega_m^2 + 0.799\omega_m \end{aligned} \quad (10)$$

$$\begin{aligned} P_h\left(u_{hh}\right) &= 2020u_{hh}^5 - 194.696u_{hh}^4 - \\ &\quad -4283.15u_{hh}^3 + 262.27u_{hh}^2 + 3796.83u_{hh} \end{aligned} \quad (11)$$

$$\begin{aligned} F_h\left(\omega_t\right) &= 9.496\cdot10^{-12}\omega_t^5 - 9.844\cdot10^{-9}\omega_t^4 + \\ &\quad +2.785\cdot10^{-7}\omega_t^3 + 1.730\cdot10^{-4}\omega_t^2 + 0.729\omega_t \end{aligned} \quad (12)$$

3) Cross coupling transfers

The cross coupling can be observed in the Twin Rotor MIMO System. The rotation of the tail motor slightly affects elevation angle while main motor strongly affects not only elevation but also azimuth. The influence of tail motor to elevation was modeled as linear function of tail rotor rotations.

The dependence of azimuth on rotations of the main motor is more complicated to model. An exponential function of the M_{v2} moment was used to cope with this problem. A Simulink scheme of this relation is presented in Fig. 3.

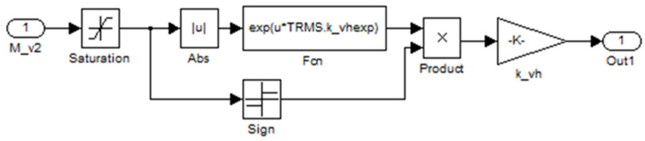

Fig. 3. Model of influence of main motor to the azimuth.

4) Cableways

A cableway between the fixed base of the Twin Rotor MIMO System and its beam plays a significant role especially in case of low rotation speed of the tail motor. Due to the cable way the system does not behave as an integrative but proportional behavior can be observed. The effect of the cableway is modelled as a nonlinear function of the azimuth.

IV. Design of robust controller

A design of robust controllers for the Twin Rotor MIMO System is based on parametric uncertainty approach. The parametric uncertainty can be used for both continuous-time and discrete systems [16].

The controlled plant was analyzed to obtain an interval uncertainty of the linear model of the system. For the control purposes, the Twin Rotor MIMO System was considered as two independent systems

- control voltage of the main rotor (input) – elevation (output)
- control voltage of the tail rotor (input) – azimuth (output)

The cross-couplings are considered as disturbances in this case.

Various step changes of the control input were applied to the plant, time responses of plant were measured and corresponding linear models were identified.

A. Identification of main rotor – elevation subsystem

Step changes of the control voltage of main rotor usually lead an oscillatory response of the elevation output. This system was modeled by a 3rd order linear system:

$$G_h(s) = \frac{b_{0h}}{a_{3h}s^3 + a_{2h}s^2 + a_{1h}s + 1} \quad (13)$$

Identification was performed in least squares sense using MATLAB function fminsearch. Results are summarized in Table I.

TABLE I. INTERVALS OF THE MAIN ROTOR – ELEVATION MODEL

Parameter	Minimal value	Maximal value
b_{0h}	60	157
a_{3h}	0.23	1.30
a_{2h}	0.22	2.35
a_{1h}	0.81	2.74

Common notation for writing transfer functions of systems with interval uncertainties uses square brackets:

$$G_h(s) = \frac{[60; 157]}{[0.23; 1.30]s^3 + [0.22; 2.35]s^2 + [0.81; 2.74]s + 1} \quad (14)$$

Model behavior especially its stability is defined by position of transfer function poles – i.e. roots of the denominator. The interval model was obtained from 29 linear models which were identified from step responses. Poles of these 29 models are presented in Fig. 4. The poles are marked by asterisk and poles of each model are connected by a line.

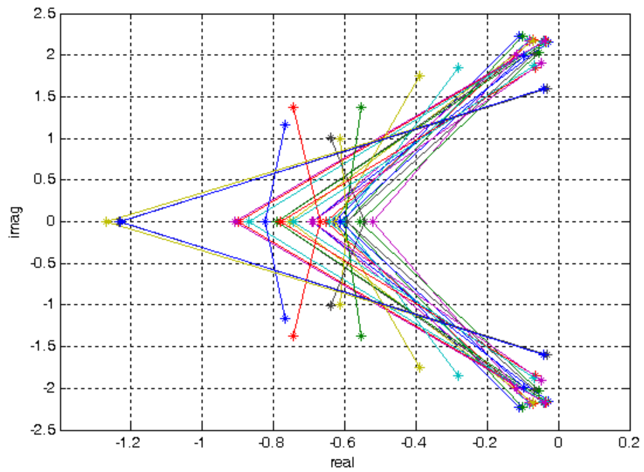

Fig. 4. Poles of the main rotor – elevation models

It can be seen that all models are stable (real parts are smaller than zero). Moreover all models are oscillatory because each model has a pair of complex conjugated poles.

Intervals of denominator of the interval model (14) form a box in the 3D space. Contrary to experiments not all transfer functions formed from the parameters inside this box are stable. The situation is presented in Fig. 5.

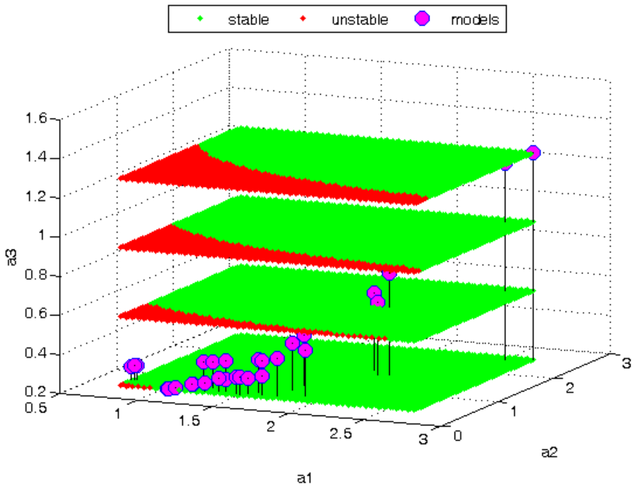

Fig. 5. Stability of interval model of the main rotor – elevation subsystem

Four crosscuts of the box are presented. The crosscuts are parallel to a_{1h} x a_{2h} plane. The upper and the lower crosscut correspond to the maximal and the minimal value of the a_{3h} parameter respectively. The other two crosscuts correspond to one third and two thirds between the minimum and maximum of a_{3h}. The red areas correspond to unstable systems while green areas correspond to stable systems. The magenta circles correspond to models identified from step responses.

B. Identification of tail rotor – azimuth subsystem

The tail rotor – azimuth subsystem was identified in the similar way as the main rotor – elevation subsystem. The main difference consists in fact that 2nd order models were used, because their accuracy was good enough.

$$G_v(s) = \frac{b_{0v}}{a_{2v}s^2 + a_{vt}s + 1} \quad (15)$$

The step responses where the plant reached a backstop were omitted from the identification. The positions of poles are presented in Fig. 6. As all the poles presented in Fig. 6 are in the left half-plane, all the models are stable and most of them are oscillatory. Limits of the model parameters are summarized in Table II.

TABLE II. INTERVALS OF THE TAIL ROTOR – AZIMUTH MODEL

Parameter	Minimal value	Maximal value
b_{0v}	75	716
a_{2v}	2.63	6.04
a_{1v}	2.49	4.55

Resulting interval model can be written in the following form:

$$G_v(s) = \frac{[75;\ 716]}{[2.63;\ 6.04]s^2 + [2.49;\ 4.55]s + 1} \tag{16}$$

Intervals of the denominator define a rectangle in a_{1v} x a_{2v} plane. As the denominator is a 2nd order degree polynomial and both a_{1v}, a_{2v} are always positive roots of denominator have always negative real part and therefore all the models are stable. Some of the models are oscillatory while the others are aperiodic. The situation is presented in Fig. 7. The magenta circles correspond to models identified from step responses.

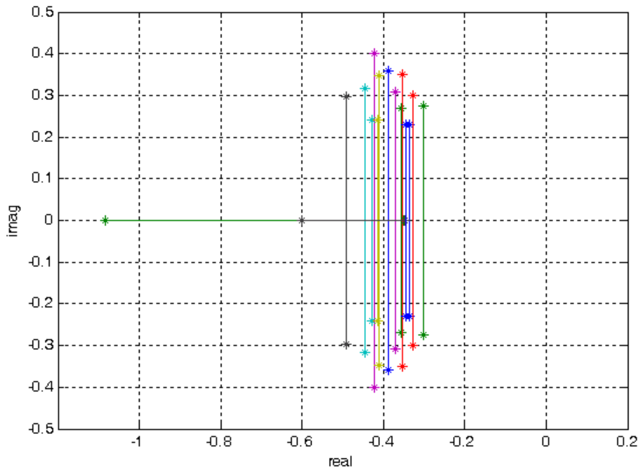

Fig. 6. Poles of the tail rotor – azimuth models

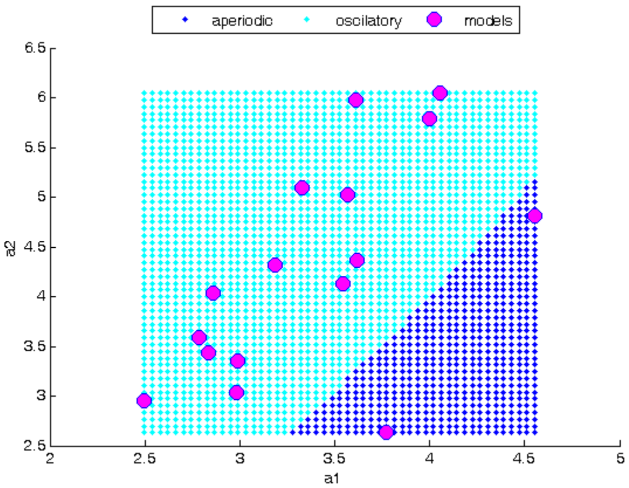

Fig. 7. Behavior of interval model of the tail rotor – azimuth subsystem

C. Design of robust 2DOF controller

Several controller types were tested and results of the 2DOF (Two Degree Of Freedom) controllers are presented in this paper. The scheme of the control loop with 2DOF controller is presented in Fig 8.

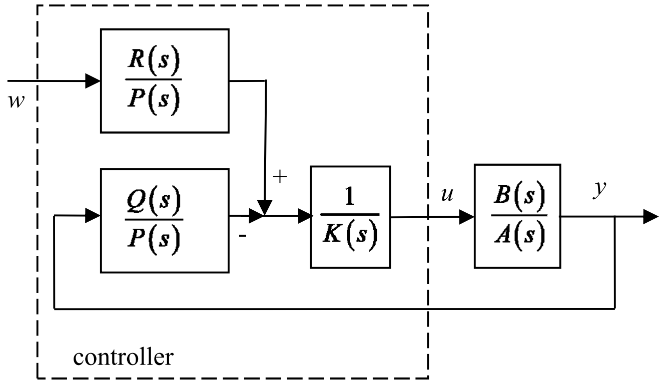

Fig. 8. 2DOF controller

Control signal is calculated according to the following equation:

$$\begin{aligned} U(s) &= \frac{1}{K(s)}\left[\frac{R(s)}{P(s)}W(s) - \frac{Q(s)}{P(s)}Y(s)\right] = \\ &= G_R(s)W(s) - G_Q(s)Y(s) \end{aligned} \tag{17}$$

where $U(s)$, $W(s)$, and $Y(s)$ are Laplace transforms of $u(t)$, $w(t)$, and $y(t)$ signals respectively. Pole-placement method was used to calculate controllers' polynomials $R(s)$, $P(s)$, $Q(s)$ and $K(s)$. Detail can be found for example in [1].

Pole placement method is based on fixing poles of closed loop to the desired positions. For robust control of a system with interval uncertainties the controller is required to guarantee stability of closed loop for any combination of parameters from the given intervals. Unfortunately coefficients of the characteristic polynomial of the closed loop are not independent. Therefore Kharitonov polynomials cannot be used for stability testing [17].

Solving the robust closed loop stability is theoretically complicated task. Hence simplified approach was used:

1. Controller polynomials were calculated with respect to given position of poles and a nominal system.
2. Coefficient values equally spread through an interval were generated for each uncertainty interval.
3. Stability of the closed loop was tested for each combination of coefficient values.

Coefficients of the nominal system were defined as midpoints of the uncertainty intervals. Five coefficient values were generated for each interval. It leads to 5^4=625 combinations (systems) for the main rotor – elevation subsystem and 5^3=125 combinations (systems) for the tail rotor – azimuth subsystem.

Pole positions were defined in the simplest possible way. One multiple real pole was used. Hence the characteristic polynomial of the closed loop has the following form:

$$D(s) = (s + \alpha)^n \tag{18}$$

Whole task of computing the robust controller can be seen as an optimization problem with the goal of stabilizing all the generated systems and the pole position as a tuning parameter.

This approach does not guarantee stability of all possible coefficient combinations but its results in real-time environment were good no unstable behavior of the closed loop was observed.

V. Real-Time Experiments

This section presents several real-time experiments from a huge set of experiments performed. A sampling period of T_0 = 0.01s was used for sensors and actuators in all experiments. Elevation control and azimuth control was performed simultaneously to verify effect of cross-couplings.

Control design consists in funding optimal position of the closed loop poles – i.e. find optimal coefficient α presented in equation (18). The goal of the optimization procedure was to stabilize all the 625 systems for the main motor – elevation subsystem and all 125 systems for the tail motor – azimuth subsystem as mentioned in the previous section.

Optimal value of pole position for elevation control was $\alpha_v = 2.7391$ (i.e. multiple pole in position -2.7391) and optimal value for azimuth control was $\alpha_h = 0.6$ (i.e. multiple pole in position -0.6). Courses of elevation control are presented in Fig. 9. Control of both real-time plant and nonlinear model derived in Section 3 are presented.

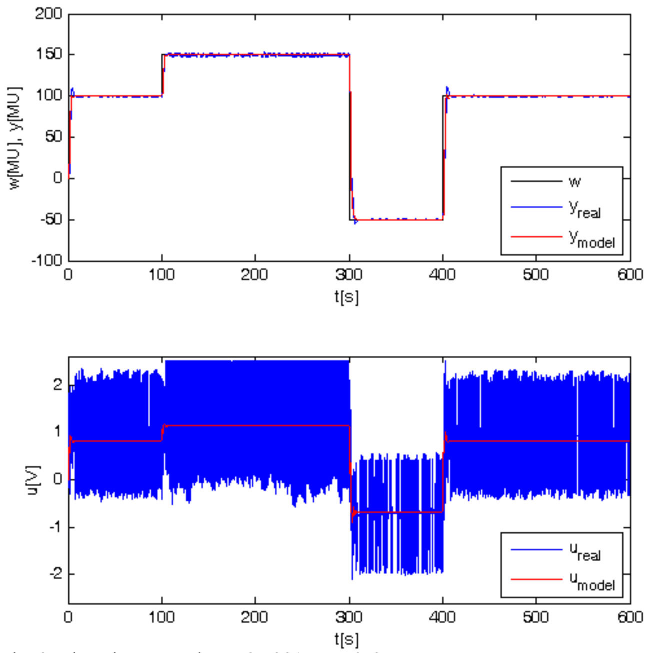

Fig. 9. Elevation control α_v = 2.7391, α_h = 0.6

It can be seen that a very good reference tracking was reached but course of control signal was very oscillatory in real-time conditions contrary to simulation.

Courses of azimuth control are presented in Fig. 10. Control of both real-time plant and nonlinear model derived in Section 3 are presented.

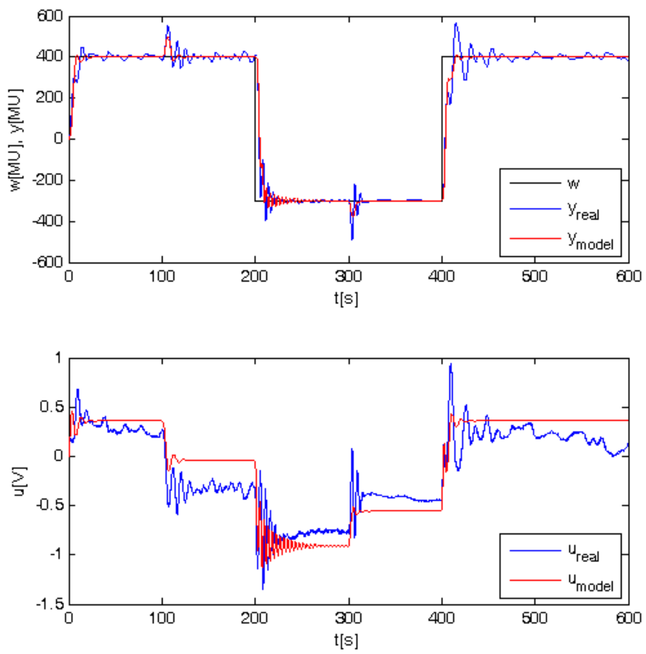

Fig. 10. Azimuth control α_v = 2.7391, α_h = 0.6

It can be observed, that cross-coupling plays important role in the azimuth control.

Pole position defined by parameter α_v was changed to obtain smoother course of control signal for the main motor. A value of α_v= 1.7 was used and the control courses of the elevation control are presented in Fig. 11.

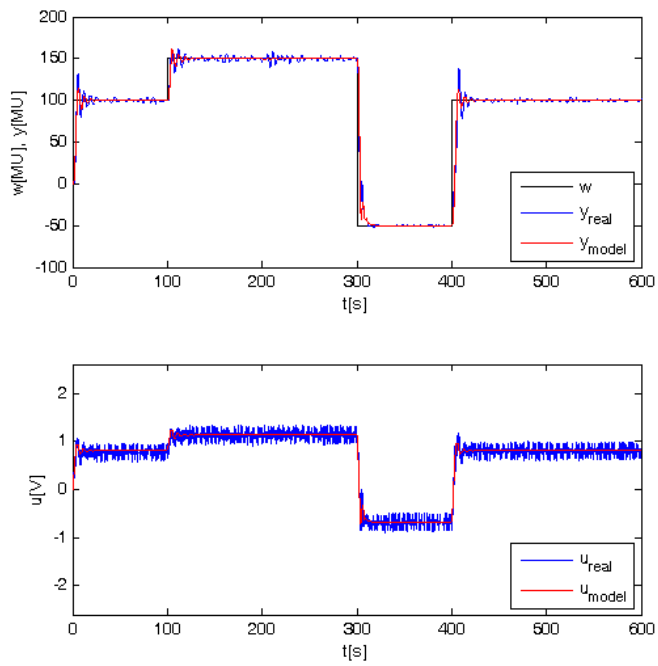

Fig. 11. Elevation control α_v = 1.7, α_h = 0.6

Reference tracking was slightly worse comparing to Fig. 9 but course of control signal was much smoother.

Courses of azimuth control of this experiment are presented in Fig. 12.

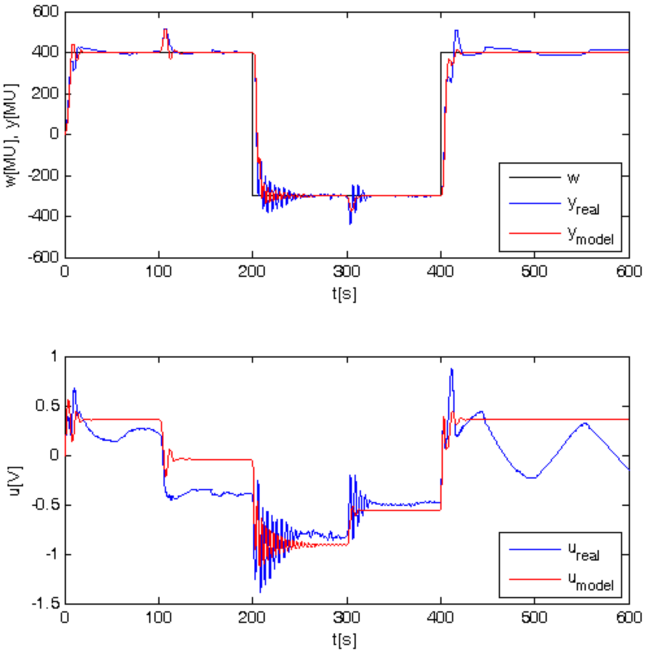

Fig. 12. Azimuth control $\alpha_v = 1.7$, $\alpha_h = 0.6$

A satisfactory control behavior with a good reference tracking was observed. The greatest difference between nonlinear model and real-time plant was obtained for control signal of the tail rotor where non-modeled behavior was observed.

Control courses were compared not only by a visual comparison of figures but also by quadratic criteria. The results are presented in Table III.

TABLE III. COMPARISON OF CONTROL COURSES

Controller	Elevation		Azimuth	
	$\sum e^2$	$\sum \Delta u^2$	$\sum e^2$	$\sum \Delta u^2$
$\alpha_v = 2.7391$ Simulation (Fig. 9, Fig. 10)	1.2470e+7	0.0707	4.3537e+8	0.0193
$\alpha_v = 1.7$ Simulation (Fig. 11, 12)	1.9766e+7	0.0206	4.5529e+8	0.0211
$\alpha_v = 2.7391$ Real plant (Fig. 9, Fig. 10)	1.3246e+7	3.4017e+3	4.5479e+8	0.2325
$\alpha_v = 1.7$ Real plant (Fig. 11, 12)	1.9948e+7	42.2463	4.5542e+8	0.1557

In real-time experiments, changing a value of the parameter α_v led to lower values of criterion which sums squares of control signal differences while reference tracking criterion remained almost unchanged.

VI. CONCLUSION

A model of nonlinear real time system Twin Rotor MIMO System was derived using first principle modeling and then enhanced to correspond better with the real plant.

A simple robust control technique was presented and successfully verified in real-time conditions. Further improvement can be acquired by implementing better pole placement. Usage of several different poles would lead to even better control courses than the courses presented in the paper.

Further work will be focused on obtaining even better performance of a robust control and subsequent comparison of results of a robust control and an adaptive control. Moreover, the presented model will be used to design and verify model based predictive control of the Twin Rotor MIMO System.

REFERENCES

[1] V. Bobál, J. Böhm, J. Fessl and J. Macháček. *Digital Self-tuning Controllers: Algorithms, Implementation and Applications*. London: Springer-Verlag, 2005.

[2] G. P. Liu, *Nonlinear identification and control – A neural network Approach*. London: Springer-Verlag, 2001.

[3] L. Ljung, *System identification: theory for the user*. Upper Saddle River, NJ: Prentice Hall PTR, 1999.

[4] J. Mikleš and M. Fikar. *Process modelling, identification, and control*. Berlin: Springer-Verlag, 2007.

[5] B. Codrons, *Process modelling for control: a unified framework using standard black-box techniques*. London: Springer-Verlag, 2005.

[6] D. M. Himmelblau and J. B. Riggs, *Basic principles and calculations in chemical engineering*. Upper Saddle River, N.J.: Prentice Hall, 2004.

[7] K.C. Tan and Y. Li, "Grey-box model identification via evolutionary computing", *Control Engineering Practice*, vol. 10, pp. 673–684, 2002.

[8] Feedback Instruments, *Twin Rotor MIMO System 33-007-PCI*, Crowborough, 2013.

[9] M. Morari and E. Zafiriou. *Robust process control*. Englewood Cliffs, N.J.: Prentice Hall, 1989.

[10] R. S. Sánchez-Peña and M. Sznaier. *Robust systems theory and applications*. New York: Wiley, 1998.

[11] *Twin Rotor MIMO*. Feedback [online]. Available: http://www.feedback-instruments.com/products/education/control_instrumentation/twin_rotor_mimo.

[12] Feedback, *Twin Rotor Mimo System – Advanced Teaching Manual 1 – 33-007-4M5*.

[13] D. Rotondo, F. Nejjari and V. Puig, "Quasi-LPV modeling, identification and control of a twin rotor MIMO system", *Control Engineering Practice*, vol. 21, pp. 829–846, 2013.

[14] A. Rahideha, M.H. Shaheed and H. J.C. Huijberts, "Dynamic modelling of a TRMS using analytical and empirical approaches", *Control Engineering Practice*, vol. 16, pp. 241–259, 2008.

[15] P. Chalupa, J. Přikryl and J. Novák "Modelling of Twin Rotor MIMO System", *Procedia Engineering*, vol. 100, pp. 249–258, 2015.

[16] R. Matušů "Robust Stability Analysis of Discrete-Time Systems with Parametric Uncertainty: A Graphical Approach", *International Journal of Mathematical Models and Methods In Applied Sciences*, vol. 8, pp. 95-102, 2014.

[17] R. Matušů and R. Prokop. "Control of Interval Systems Using 2DOF Configuration", *Procedia Engineering*, vol. 100, pp. 340 – 344, 2015.